
Masters Theses

Student Theses and Dissertations

Summer 2009

Oxidative stress, calcium homeostasis, and altered gene expression in human lung epithelial cells exposed to ZnO nanoparticles

Chuan-Chin Huang

Follow this and additional works at: https://scholarsmine.mst.edu/masters_theses



Part of the [Biology Commons](#), and the [Environmental Sciences Commons](#)

Department:

Recommended Citation

Huang, Chuan-Chin, "Oxidative stress, calcium homeostasis, and altered gene expression in human lung epithelial cells exposed to ZnO nanoparticles" (2009). *Masters Theses*. 93.

https://scholarsmine.mst.edu/masters_theses/93

This thesis is brought to you by Scholars' Mine, a service of the Missouri S&T Library and Learning Resources. This work is protected by U. S. Copyright Law. Unauthorized use including reproduction for redistribution requires the permission of the copyright holder. For more information, please contact scholarsmine@mst.edu.

**OXIDATIVE STRESS, CALCIUM HOMEOSTASIS, AND ALTERED GENE
EXPRESSION IN HUMAN LUNG EPITHELIAL CELLS EXPOSED TO ZnO
NANOPARTICLES.**

by

Chuan-Chin Huang

A THESIS

**Presented to the Faculty of the Graduate School of the
MISSOURI UNIVERSITY OF SCIENCE AND TECHNOLOGY**

In Partial Fulfillment of the Requirements for the Degree

MASTER OF SCIENCE IN ENVIRONMENTAL BIOLOGY

2009

Approved by

**Yue-wern Huang, Advisor
Robert S. Aronstam
Paul Nam**

© 2009

Chuan-Chin Huang

All Rights Reserved

PUBLICATION THESIS OPTION

This thesis has been prepared in the form for publication in the journal of
Toxicology in Vitro.

ABSTRACT

The influence of 20 nm ZnO nanoparticles on oxidative stress, intracellular calcium homeostasis, and gene expression was studied in human bronchial epithelial cells (BEAS-2B). ZnO caused a concentration- and time-dependent cytotoxicity while elevating oxidative stress and causing membrane damage (cellular LDH release). There was a remarkably steep relationship between concentration and toxicity at concentrations from 5 to 10 $\mu\text{g/ml}$. Exposure to ZnO increased intracellular calcium levels in a concentration- and time-dependent manner. Treatment with the antioxidant *N*-acetylcysteine prevented cell loss and diminished the increase in intracellular calcium concentration, suggesting oxidative stress mediated cytotoxicity. Exposure to a sublethal concentration of ZnO increased the expression of BNIP, PRDX3, PRNP, and TXRND1 genes by at least or above 2.5 fold. These four genes are involved in apoptosis and oxidative stress responses.

ACKNOWLEDGMENTS

I would like to express my gratitude to my graduate advisor, Dr. Yue-wern Huang. His guidance and knowledge were the basis for the work here presented and the comments and extended hours that he dedicated to help me during my graduate study life are invaluable. I also would like to thank my committee members, Dr. Robert Aronstam and Dr. Paul Nam for all their support, advice and comments on the research. Also, I would like to say many thanks to Dr. Kate Shannon and Dr. Nathen Chen, for all the help and advices. I also would like to say thank you to Connie Behrick, Kluesner Rachel and Pelc Jessica, for all the help.

To my co-workers and very special friends, Yi Xu and Gregory Schmoll, thank for your help in the lab. To my good friend, Xin Sheng Zhang, thank for your help and encouragement. To Martin Adam and Hsu Jen Wang, thanks for your kindly help in lab facility. To all my friends at MST, thank you for all support over these years.

I wish to express my gratitude to CDNA Center in Missouri University in Science and Technology that provided the funds for my research.

And very special thanks to my family and friends in Taiwan, thank for their support, patience through this process.

TABLE OF CONTENTS

	Page
PUBLICATION THESIS OPTION.....	iii
ABSTRACT.....	vi
ACKNOWLEDGMENTS	v
LIST OF ILLUSTRATIONS.....	vii
LIST OF TABLES.....	viii
PAPER	
1. OXIDATIVE STRESS, CALCIUM HOMEOSTASIS, AND ALTERED GENE EXPRESSION IN HUMAN LUNG EPITHELIAL CELLS EXPOSED TO ZNO NANOPARTICLES.....	1
1.1. ABSTRACT.....	2
1.2. INTRODUCTION	3
1.3. MATERIALS AND METHODS.....	4
1.4. RESULTS	10
1.5. DISCUSSION	13
1.6. ACKNOWLEDGEMENT	17
1.7. REFERENCES	18
VITA	37

LIST OF ILLUSTRATIONS

Figure	Page
1.1. Characterization of ZnO oxide nanoparticles	28
1.2. Dose-response curve and ROS level	29
1.3. Correlation between ROS level and cell viability	30
1.4. LDH activity	31
1.5. Correlation between LDH and ROS	32
1.6. NAC recoverary.....	33
1.7. Gene expression alteration.....	34
1.8. Calcium modulation	35
1.9. Correlation between calcium and cell viability	36

LIST OF TABLES

Table	Page
1.1. Impurity of ZnO nanoparticles	24
1.2. Gene table	25

**OXIDATIVE STRESS, CALCIUM HOMEOSTASIS, AND ALTERED GENE
EXPRESSION IN HUMAN LUNG EPITHELIAL CELLS EXPOSED TO ZnO
NANOPARTICLES**

Chuan-Chin Huang^{*}, Robert S. Aronstam[†], Da-Ren Chen[‡], Yue-wern Huang^{*}

^{*}Department of Biological Sciences, Missouri University of Science and Technology, 105
Schrenk Hall, 400 W. 11th Street, Rolla, MO 65409

[†]Department of Biological Sciences and M S&T cDNA Resource Center, Missouri
University of Science and Technology, 105 Schrenk Hall, 400 W. 11th Street, Rolla, MO
65409

[‡]Department of Energy, Environmental and Chemical Engineering, Washington
University in St. Louis, Campus Box 1180, One Brookings Drive, St. Louis, MO 63130

Corresponding Author:
Yue-wern Huang, Ph.D.
Department of Biological Sciences
Missouri University of Science and Technology
Tel: 573-341-4589
Fax: 573-341-4821
E-Mail: huangy@mst.edu

1.1. ABSTRACT

The influence of 20 nm ZnO nanoparticles on oxidative stress, intracellular calcium homeostasis, and gene expression was studied in human bronchial epithelial cells (BEAS-2B). ZnO caused a concentration- and time-dependent cytotoxicity while elevating oxidative stress and causing membrane damage (cellular LDH release). There was a remarkably steep relationship between concentration and toxicity at concentrations from 5 to 10 $\mu\text{g/ml}$. Exposure to ZnO increased intracellular calcium levels in a concentration- and time-dependent manner. Treatment with the antioxidant *N*-acetylcysteine prevented cell loss and diminished the increase in intracellular calcium concentration, suggesting oxidative stress mediated cytotoxicity. Exposure to a sublethal concentration of ZnO increased the expression of BNIP, PRDX3, PRNP, and TXRND1 genes by at least or above 2.5 fold. These four genes are involved in apoptosis and oxidative stress responses. Clearly ZnO affects transcriptional regulation in exposed cells. In summary, exposure of BEAS-2B cells to 20 nm ZnO particles results in 1) a concentration- and time- dependent cytotoxicity reflected in cell viability reduction, elevated oxidative stress, and cell membrane damage; 2) a concentration- and time-dependent elevation of intracellular calcium levels; and 3) up-regulation of several genes relevant to oxidative stress responses and apoptosis. The relationship between the altered expression of the redox-sensitive genes and the altered calcium levels is currently under investigation.

Key words: nanoparticles, ZnO, oxidative stress, calcium modulation, gene expression

1.2. INTRODUCTION

Nanomaterials are materials that have at least one dimension in the range of 1-100 nm. Due to their unique physical and chemical characteristics, nanomaterials have become widely used as the production of cosmetic products, transparent conductive, paints and filters. Unintended exposure to nanomaterials may occur in occupational workers and end product users via inhalation, dermal absorption, or gastrointestinal tract absorption. Nanomaterials are thought to impose more serious adverse effects on organisms than micro-scale materials because of their smaller sizes and corresponding larger-specific surface areas (Kipen and Laskin, 2005; Oberdorster *et al.*, 2005; Nel *et al.*, 2006). We and others have studied the differential adverse effects of nanomaterials with various properties on human health *in vitro* and *in vivo* settings (Timblin *et al.*, 2002; Li *et al.*, 2003; Braydich-Stolle *et al.*, 2005; Gurr *et al.*, 2005; Moller *et al.*, 2005; Jeng and Swanson, 2006; Lin *et al.*, 2006b; Lin *et al.*, 2006a; Wagner *et al.*, 2007; Kang *et al.*, 2008; Lewinski *et al.*, 2008; Lin *et al.*, 2008a; Lin *et al.*, 2008b)

Nanostructures of ZnO, including particles, rods, wires, belts, tubes, cages, walls, and rings, have attracted much attention due to their unique electronic and optoelectronic properties at nanoscale levels and novel applications in catalysis, paints, wave filters, UV detectors, transparent conductive films, varistors, gas sensing, solar cells, sunscreens, and other cosmetic products (Comini *et al.*, 2002; Bai *et al.*, 2003; Ramakrishna, 2003; Bae and Seo, 2004; Ding and Wang, 2004; Zhu *et al.*, 2005; Huang *et al.*, 2006). Inhalation of ZnO compromises pulmonary function in pigs and pulmonary impairment and metal fume fever in humans (Fine *et al.*, 1997; Beckett *et al.*, 2005). In our previous study, exposure of human bronchial carcinoma-derived cells (A549) to nano- and micro-

size ZnO particles caused much steeper dose-dependent cytotoxicity relationships than those seen with other metal oxides (Lin *et al.*, 2008b). In Mechanistic studies suggested that the toxicity reflected elevated oxidative stress (OS) and oxidative DNA damage. In a single dosage, time-dependent study by Xia *et al.*, ZnO (13nm) induced toxicity in RAW 274.7 and BEAS-2B cell lines, leading to generation of reactive oxygen species, excitation of inflammation, and cell death (Xia *et al.* 2008).

In the present study, we extended our studies to include a consideration of ZnO-mediated changes in cellular pathway-specific gene expression associated with oxidative stress and antioxidant defense in immortalized human normal bronchial epithelial cells (BEAS-2B). Further, the relationship among OS, intracellular calcium ($[Ca^{2+}]_{in}$) concentration, and cell viability was delineated. Accordingly, the specific objectives of this study were to understand the relationships between the following responses of immortalized human normal bronchial epithelial cells (BEAS-2B) to ZnO nanoparticles: 1) cytotoxicity, 2) mechanism of cytotoxicity, 3) expression of OS responsive genes, and 4) intracellular calcium homeostasis.

1.3. Materials and Methods

ZnO particles characterization

Twenty nanometer ZnO particles at > 99% purity were purchased from Nanostructured and Amorphous Materials (Los Alamos, New Mexico, USA). We characterized particle morphology, size, and agglomeration states using scanning electron microscopy (SEM) and transmission electron microscopy (TEM). Particle size analysis was carried out by measuring specific surface area (SSA, m^2/g) with the Brunauer,

Emmett and Teller (BET) techniques (Quantachrome; Nova 1000). Corresponding X-ray diffractometry (XRD; Scintag 2000) was used to characterize particle crystallinity. The above characterizations were performed in a dry state. Impurities in nanoparticles were measured using the Inductively Coupled Plasma-Mass Spectrometer (ICP-MS; Agilent ICP_MS 7500ce with SP-5 Autosampler) with the routine elemental analysis setup. All the samples were analyzed by dispersing the powders in a 1% HNO₃ solution.

All ZnO nanoparticles suspensions were freshly prepared with medium immediately before each experiment. Suspensions were mixed vigorously and immediately applied to BEAS-2B cells to minimize precipitation. Hydrodynamic size (an indicator of agglomeration) of ZnO in BEAS-2B culture medium were characterized by a dynamic light scattering (DLS) method at 100 µg/ml (stock solution), as well as a series of dilutions to 10 µg/ml.

Chemicals

Bronchial epithelial cell basal culture medium and additional growth factors were purchased from Lonza (Basel, Switzerland). Trypsin-EDTA (1X), ROS detection reagents and Hank's balanced salt solution (HBSS) were obtained from Invitrogen (Carlsbad, CA, USA). N-acetylcysteine (NAC), penicillin-streptomycin, and Tris-HCl were purchased from Aldrich-Sigma (St. Louis, MO, USA). MTS assay kits were purchased from Promega (Madison, WI, USA). LDH assay kits were purchased from Takara (Shiga, Japan).

Cell culture and treatment with ZnO particles

The immortalized human normal bronchial epithelial cells (BEAS-2B) were purchased from ATCC (Manassas, VA, USA). These continuously cultured cells are being

widely used as an *in vitro* model for studying the prevention of the development of human lung carcinogenesis as well as nanotoxicity testing (Sharma *et al.*, 1997; Prahalad *et al.*, 2001; Park *et al.*, 2008). The working culture medium contained 500 ml BEMB basal culture medium, 0.5 ng/ml recombinant epidermal growth factor (EGF), 500 ng/ml hydrocortisone, 0.005 mg/ml insulin, 0.035 mg/ml bovine pituitary extract, 500 nM ethanolamine, 500 nM phosphoethanolamine, 0.01 mg/ml transferrin, 6.5 ng/ml 3,3', 5-triiodothyronine, 500 ng/ml epinephrine, 0.1 ng/ml retinoic acid, trace elements, 5 ml milliliters of 10,000 unit/ml penicillin plus 10,000 µg/ml streptomycin.

Cells were grown at 37° in a 5% CO₂ humidified environment. For measurement of cytotoxicity, cell membrane damage and intracellular ROS levels, approximately 4,000 cells were seeded into each well of a 96 well plate and allowed to attach and grow for 48 hours before being treated. For the gene expression study, cells were seeded into 75 cm² flasks at a 30% confluence, and then allowed to attach and grow for 48 hours before use. To reduce experimental variations and improve data accuracy, ZnO particles were dried before being weighed on an analytical balance. Various ZnO concentrations were achieved by diluting the stock suspension (100 µg /ml). Cells without ZnO particles served as controls in each experiment. Fresh medium without cells and nanoparticles were used as blanks in certain assays.

Cytotoxicity and mechanism of ZnO nanoparticles in BEAS-2B cells

To determine the cytotoxicity of 20 nm ZnO, BEAS-2B cells were treated with 5, 6, 7, 8, 9, or 10 µg/ml of ZnO. Untreated cells were used as a control group. Titanium dioxide (TiO₂), which has been shown to caused 30% cell death to BEAS-2B cells at 20 µg/ml (Park *et. al.*, 2008), was included for comparison. The MTS assay (Cell Titer 96[®]

Aqueous One Solution Assay, Promega) was used to determine cytotoxicity. Absorbance was measured at 490 nm using a microplate reader (FLOURstat; BMG Labtechnologies, Durham, NC, USA). A concentration-dependent cytotoxicity study was conducted on N-acetylcysteine to identify a sublethal level for the subsequent validation of ZnO-induced toxicity mechanism. A potential detection interference between ZnO and the dye in MTS was taken into account in order to exclude false positives.

Intracellular ROS measurement

ROS generation was measured using a more efficient derivative of 2', 7'-DCFH-DA, 5-(and-6)-carboxy-2', 7'-dichlorodihydrofluorescence diacetate (carboxy-H₂DCFDA). A H₂DCFDA stock solution of 10 mM (in ethanol) was diluted 500-fold in BEAS-2B culture medium to yield a 20 μM working solution. Cells were washed twice and then incubated with the H₂DCFDA working solution for 1 h in a dark environment (37° incubator). Then the cells were washed twice using fresh medium, followed by treatment with 20 nm ZnO particles for 24 h. Fluorescence was then determined at 485 nm excitation and 520 nm emission using a microplate reader.

LDH measurement

Release of lactate dehydrogenase (LDH) to cell culture medium indicates of cell membrane damage. LDH activity in the supernatant was determined using an LDH Kit (Takara Bio; Otsu, Shiga, Japan). One hundred microliter of cell supernatant was used for LDH analysis. LDH released by damaged cell membrane catalyzed the NAD⁺ to NADH. Thus, the rate of NAD⁺ reduction is directly proportional to LDH activity. Absorption was measured at 490 nm using a microplate reader.

Modulation of intracellular calcium concentrations ($[Ca^{2+}]_{in}$)

Fura-2, a UV-excitable fluorescent molecule, was used as a calcium indicator. To study $[Ca^{2+}]_{in}$ modulation in ZnO laden cells, approximately 20,000 cells in 3 ml culture medium were seeded in a glass bottom culture dish (MatTek, Ashland, USA). Twenty-four later, culture medium was discarded and the cells were treated for 6 h with 3 ml of new medium with the desired ZnO concentration. Forty minutes before terminating the experiment, 1.5 ml of the medium was removed for supplementation with 2 μ M fura-2 AM before being added back to the cells. The cells were incubated for 20 minutes to allow efficient loading of membrane permeable fura-2 AM and cleavage of the acetoxymethyl (AM) group by intracellular esters to yield the Ca^{2+} sensitive, membrane impermeable dye, fura 2. The entire medium was then removed and placed in the 37°C incubator while the cells were washed with fresh warm medium twice to get rid of excess fura-2 AM. Following this wash, the medium was added back to the cells for 20 minutes, and the cells allowed recovering before being exposed to ZnO for another 20 minutes. The cells were then placed on the stage of an inverted fluorescence microscope (*InCyt Basic IM* Fluorescence Imaging System, Intracellular Imaging Inc.). A dual wavelength monochromator of 340 nm and 380 nm was used to excite fura 2. Emission was monitored at 510 nm with a photomultiplier at an acquisition rate of 10 Hz per ratio, and fluorescence ratio (F_{340}/F_{380}) values were determined. Data were analyzed using InCYtlm2 software. Following exposure to 9 and 10 μ g/ml ZnO for more than six hours, most of the exposed cells appeared to be dying and were becoming detached from the bottom of the dish, preventing meaningful measurement. To investigate the role of ROS in $[Ca^{2+}]_{in}$ modulation, cells were co-treated with ZnO and the antioxidant NAC (0.1 mM).

Gene expression alteration by ZnO nanoparticles

A pathway-specific microarray comprised of probes for 84 oxidative stress and antioxidant defense relevant genes (Cat. no. PAHS-065, SuperArray Bioscience, Frederick, MD, USA) was used to investigate gene expression alteration by ZnO nanoparticles in BEAS-2B cells. After being treated with a sublethal concentration of ZnO nanoparticles (5 μ g/ml), approximately 6×10^6 cells were collected for RNA extraction using a RNeasy Mini Kit (Qiagen, Valencia, CA, USA). cDNAs were reverse transcribed from the extracted RNA using a RT² First Strand Kit (SuperArray). cDNAs were then mixed with the RT² SYBR Green/Rox PCR master mix (SuperArray) and 40 polymerase chain cycles were performed using a Mxp3000 Real-Time thermocycler (Stratagene, La Jolla, CA, USA). Five array replicates were performed. For quality assurance, human genomic DNA contamination (plate pos. no. H06), three reverse transcription controls (plate pos. no. H07, H08, H09), and three positive PCR controls (plate pos. no. H10, H11, H12) were included in each 96-well microarray plate. The housekeeping gene GAPDH (plate pos. no. H04) was used for normalization, and the data were analyzed with the $\Delta\Delta C_t$ method. The difference between the C_t values (ΔC_t) of the gene of interest and the housekeeping gene is calculated for each experimental sample. Then, the difference in the ΔC_t values between the experimental and control samples ($\Delta\Delta C_t$) is calculated. The fold-change in expression of the gene of interest between the two samples is then equal to $2^{(-\Delta\Delta C_t)}$.

More detailed annotations, array layout, and gene table can be found at <http://www.sabiosciences.com/genetable.php?pcatn=PAHS-065A>. Data analysis and manufacturer's performance data sensitivity, specificity, and reproducibility are located at

http://www.sabiosciences.com/rt_pcr_product/HTML/PAHS-065A.html#accessory.

Statistical analysis

In the toxicity studies, three independent experiments were conducted, triplicates for each treatment group. Data were expressed as mean \pm SD. In this study, we aimed at differing between-group values; thus; therefore, we selected the one-tailed unpaired Student's *t* test. The *p* value was set at 0.05. In the microarray study, each treatment group contained five replicates.

1.4. RESULTS

ZnO particle characterization

The size of primary ZnO particles measured by TEM was around 20 nm. However, the clusters of much primary particles are typically observed after the ZnO powder was dispersed. The particle specific surface area measured by BET was 47.47 m²/g. The equivalent BET diameter was 22.5 nm (density of 5.6 g/cm³ is used). X-ray diffraction (XRD) analysis revealed highly crystalline and Zincite crystal structure (**Fig. 1.1.a**). The estimated crystallite size was approximately 14 nm, based upon the three biggest peaks in the XRD spectrum. Shown in **Fig. 1.1.b** is the TEM image of ZnO particles. The SEM morphology of particle cluster is given in **Fig 1.1.c**. It is observed from both images that ZnO particles of 20nm are in fact highly agglomerated. The surface morphology of ZnO agglomerates is very random and the surface condition is mostly rough. The total purity of ZnO particle powder was greater than 97.9 % (**Table 1.1**). Elements such as Cu, Cr, Fe, V, and Co that may generate free radicals via the Fenton reaction were below detection limits (0.04 ppm). The hydrodynamic sizes, an indication of ZnO nanoparticle

agglomeration in the cell culture medium, ranged from 50 to 70 nm at ZnO concentrations between 5 and 50 $\mu\text{g/ml}$. A dramatic increase to 300 nm was observed at 100 $\mu\text{g/ml}$, indicating extensive agglomeration.

Dose- and time-dependent cytotoxicity of ZnO particles

Exposure of BEAS-2B cells to 20 nm ZnO particles showed a steep concentration-dependent cell viability reduction relationship (**Figure 1.2.a**). ZnO nanoparticle cytotoxicity was observed at concentrations as low as 5-6 $\mu\text{g/ml}$; there was a steep decline in cell numbers at concentrations between 6 and 10 $\mu\text{g/ml}$. At 5, 6, 7, 8, 9, and 10 $\mu\text{g/ml}$, ZnO decreased cell viability by approximately 4, 14, 50, 85, 92 and 96%, respectively. A time course study revealed that toxicity induced by 20 nm ZnO particles occurred within 6 h; more pronounced toxicity was observed after 24 h exposure. Positive results were excluded because the interference caused by the reaction of ZnO nanoparticles and MTS assay was not observed (data not shown).

ZnO particles induce oxidative stress and cause cell membrane damage

Intracellular ROS levels were significantly increased after 6 h and 24 h exposure to all concentrations of ZnO examined (p 's < 0.05 ; **Fig. 1.2.b**). There was an inverse correlation between ROS and cell viability ($R^2 = 0.741$; **Fig. 1.3.**). Cell membrane damage was reflected in LDH release from cells in to the culture medium. LDH levels following 24 h exposure to ZnO at 5, 6, 7, 8, 9 and 10 $\mu\text{g/ml}$ were increased by $\sim 26\%$, 31% , 34% , 60% , 100% and 133% , respectively, in comparison with the control group (p 's < 0.05 ; **Fig. 1.4.**). There was a positive correlation between LDH activity and ROS level ($R^2 = 0.953$; **Fig. 1.5.**).

N-acetylcysteine prevents cytotoxicity induced by ZnO particles

To further establish the role of oxidative stress in ZnO-induced cytotoxicity, cells were co-treated with or without an antioxidant, N-acetylcysteine (NAC). Preliminary dose response studies indicated that NAC was not toxic to BEAS-2B cells below at concentrations below 1.0 mM (data not shown). Accordingly, we used NAC at 0.1, 0.3 and 0.5 mM concentrations to co-treat with the cells exposed to ZnO at 8 µg/ml. NAC co-treatment increased cell viability by 88 %, 90 % and 92 %. This result supports OS-mediated cytotoxicity, and suggests that NAC and other antioxidants may be effective in preventing or treating injuries resulting from exposure to ZnO nanoparticles (**Fig. 1.6.**).

Pathway-specific gene expression alteration in ZnO-exposed cells

The Human Oxidative Stress and Antioxidant Defense PCR array that includes 84 OS-responsive genes is used to study potential effects on gene expression. The genes investigated are categorized as superoxide release and metabolism genes, peroxide metabolism genes, oxidoreductases genes, other genes involved in oxidative stress, inflammation related genes, apoptotic inducer genes, and cell cycle related genes. A sublethal, but ROS-elevating concentration of ZnO (5 µg/ml) was used to avoid interference from disruption of intermediary metabolism, bioenergetics, and cell structure. Changes in gene expression in the ZnO-treated cells relative to control for a 24 h exposure paradigm are presented in Table 2. The expressions of BNIP3 (BCL2/adenovirus interacting protein 3), PRDX3 (peroxiredoxin 3), PRNP (Prion protein), and TRXND1 (thioredoxin reductase 1) were elevated by at least 2.5-fold above control levels (**Fig. 1.7.**).

Alterations of intracellular calcium levels in ZnO-exposed cells

To understand influence of oxidative stress on calcium homeostasis and to delineate

relationship among oxidative stress, calcium homeostasis, and cell viability, a time- and dose-dependent study was carried out to measure intracellular calcium levels. Dose dependent increases in $[Ca^{2+}]_{in}$ was observed in cells exposed to ZnO for 6 h (**Fig. 1.8.**). At 9 and 10 $\mu\text{g/ml}$ of ZnO, $[Ca^{2+}]_{in}$ increased by 230% and 370% above control levels, respectively. The antioxidant NAC partially attenuated the increases in $[Ca^{2+}]_{in}$ to levels 140% and 190% above control levels, respectively. There was an inverse correlation between $[Ca^{2+}]_{in}$ and cell viability ($R^2 = 0.952$; **Fig. 1.9.**).

1.5. DISCUSSION

In a previous study we showed that exposure of A549 cells to 70 nm and 420 nm ZnO resulted in much steeper dose-cytotoxicity relationships (8 $\mu\text{g/ml}$ – 18 $\mu\text{g/ml}$) than those seen with other metal oxides particles, including Al_2O_3 , TiO_2 , and CeO_2 (Lin *et al.*, 2006b; Lin *et al.*, 2006a; Lin *et al.*, 2008a; Lin *et al.*, 2008b). In the present study, exposure of BEAS-2B cells to 20 nm ZnO particles also resulted in a steep dose-response relationship, with little toxicity seen at 5 $\mu\text{g/ml}$ and almost complete cell death at 10 $\mu\text{g/ml}$ (24 h exposure). Thus, the steep dose-cytotoxicity phenomenon associated with ZnO particles is not cell line-dependent. However, ZnO (20 nm) is somewhat more toxic to BEAS-2B cells than to A549 cells (data not shown).

ZnO (20 nm)-induced cytotoxicity was time dependent; the toxicity developed within 6 hours, and was more pronounced response after a 24 h exposure. OS was elevated at all levels of ZnO concentrations, with a greater increase with the longer exposure. General correlation analyses among ROS, LDH, and cell viability suggest that elevated OS damage cell membrane leading to cell death (Fig 2c & 3b). On the other hand,

concentration specific analyses reveal that OS and cell membrane damage occur under exposure conditions (5 & 6 $\mu\text{g}/\text{ml}$, 24 h) that do not cause cytotoxicity.

Intracellular calcium concentration ($[\text{Ca}^{2+}]_{\text{in}}$) has major effects on cellular metabolism, signal transduction, and gene expression. $[\text{Ca}^{2+}]_{\text{in}}$ is tightly regulated, and alteration of $[\text{Ca}^{2+}]_{\text{in}}$ is associated with cellular dysfunction, metabolic and energetic imbalance, disease states, and cell death. A host of environmental toxicants elevate $[\text{Ca}^{2+}]_{\text{in}}$ directly or indirectly by promoting Ca^{2+} influx, releasing Ca^{2+} from intracellular stores, or inhibiting Ca^{2+} efflux from the cell. In the present study, we evaluated alteration of intracellular calcium homeostasis immediately after exposing cells to ZnO. No substantial change was observed in the first hour of exposure. However, a 6-hour exposure to ZnO caused a concentration-dependent elevation of $[\text{Ca}^{2+}]_{\text{in}}$, which could be partially attenuated by antioxidant NAC indicating calcium homeostasis is oxidative stress responsive. Further, the inverse correlation between $[\text{Ca}^{2+}]_{\text{in}}$ and cell viability indicates a role for calcium in cell death. Presumably, ZnO may interact with certain intracellular biomolecules to generate ROS/RNS which can oxidatively inactivate the thiol-dependent Ca^{2+} pump, leading to an accumulation of Ca^{2+} in the cytosol. The accumulated Ca^{2+} would be expected to further elevate ROS/RNS via involvement of Ca^{2+} -activated proteases, dehydrogenases, etc. Attenuation of $[\text{Ca}^{2+}]_{\text{in}}$ by NAC to levels \approx 50% higher than the normal was sufficient to prevent cell death.

Oxidative stress can affect multiple signaling pathways, including those of NF- κ B, p38 MAPK, JNK/SAPK, hexosamine, PKC, AGE/RAGE, sorbitol (Evans *et al.*, 2002). Since ZnO was observed to increase OS, we assessed the ability of ZnO to modulate the expression of stress responsive genes. In order to avoid interfere with ZnO effects on

intermediary metabolism, bioenergetics and cell structures, we selected a sublethal concentration of ZnO which reliably increase ROS. The expression of four genes was altered in the ZnO-treated cells. BNIP3 (BCL2/adenovirus E1B 19kDa interacting protein 3) contains a BH3 domain and a transmembrane domain, which have been associated with pro-apoptotic activity. The dimeric mitochondrial protein encoded by this gene induces apoptosis (Wan *et al.*, 2003). PRDX3 (peroxiredoxin 3) belongs to the family of Peroiredoxin (Prx) enzymes that are thought to relieve cells from OS by removing the low levels of hydroperoxides produced during normal cellular metabolism. PRDX3 encodes a protein with antioxidant functions that is localized in the mitochondrion (Jeong *et al.*, 2006). PRNP (Prion protein) are important in regulating glutathione reductase (GR) activity (White *et al.*, 1999). Because GR functions in the regeneration of cellular GSH (glutathione), lower GR activity would decrease the breakdown of oxidants by glutathione (Vassallo and Herms, 2003). TRXND1 (thioredoxin reductase 1) encodes a member of the family of pyridine nucleotide oxidoreductases that plays a role in selenium metabolism and protection against oxidative stress (Hintze *et al.*, 2003). In summary, exposure of BEAS-2B cells to a sublethal concentration of ZnO nanoparticles induced the expression of four genes involved in oxidative stress and apoptosis, which was in agreement with the findings with biochemistry and cytotoxicity. The most important point to observe here is that the apoptotic inducer, BNIP3, has been turned on with a sublethal dose of ZnO particles, suggesting that apoptosis directly reflects the cytotoxicity of ZnO nanoparticles. To our surprise, expression of the commonly known antioxidant genes such as catalase, glutathione peroxidase, glutathione reductase, glutathione transferase, and superoxide dismutase were not significantly upregulated in

cells exposed to ZnO. However, this finding is consistent with results obtained with toxic single-walled carbon nanotubes in BJ Foreskin cells (Sarkar *et al.*, 2007).

We have demonstrated that 20 nm ZnO particles reduce the viability of in human bronchial epithelial cells (BEAS-2B) while elevating oxidative stress and cell membrane damage in a concentration- and time-dependent fashion. Intracellular calcium concentration was increased in response to ZnO exposure, and this increase was correlated with reduced cell viability and it could be partially reversed by treatment with an antioxidant. Exposure to a sublethal concentration of ZnO nanoparticles altered the expression of several genes that are involved in oxidative stress and apoptosis.

1.6. ACKNOWLEDGEMENT

This work is supported by the Department of Biological Sciences and the cDNA Resource Center at the Missouri University of Science and Technology. The authors thank Yi Xu and Greg Schmoll for technical support.

1.7. REFERENCES

- Bae, S. Y., and Seo, H. W., 2004. Vertically aligned sulfur-doped ZnO nanowires synthesized via chemical vapor deposition. *Journal of Physical Chemistry* 108, 5206-5210.
- Bai, X. D., Gao, P. X., Wang, Z. L., and Wang, E. G., 2003. Dual-mode mechanical resonance of individual ZnO nanobelts. *Applied Physical Letter* 28, 4806-4808.
- Beckett, W. S., Chalupa, D. F., Pauly-Brown, A., Speers, D. M., Stewart, J. G., Frampton, M. W., Utell, M. J., Huang, L. S., Cox, C., Zareba, W., and Oberdorster, G., 2005. Comparing inhaled ultrafine versus fine zinc oxide particles in healthy adults: a human inhalation study. *American Journal of Respiratory and Critical Care Medicine* 171, 1129-1135.
- Braydich-Stolle, L., Hussain, S., Schlager, J. J., and Hofmann, M. C., 2005. In Vitro Cytotoxicity of Nanoparticles in Mammalian Germline Stem Cells. *Toxicological Science* 88, 412-419.
- Comini, E., Faglia, G., Sberveglieri, G., Pan, Z., and Wang, Z. L., 2002. Stable and highly sensitive gas sensors based on semiconducting oxide nanobelts. *Applied Physics Letter* 81, 1869-1871.
- Ding, Y., and Wang, Z. L., 2004. Structure analysis of nanowires and nanobelts by transmission electron microscopy. *Journal of Physical Chemistry* 108, 12280-12291.
- Evans, J. L., Goldfine, I. D., Maddux, B. A., and Grodsky, G. M., 2002. Oxidative stress and stress-activated signaling pathways: a unifying hypothesis of type 2 diabetes. *Endocrine Reviews* 23, 599-622.

- Fine, J. M., Gordon, T., Chen, L. C., Kinney, P., Falcone, G., and Beckett, W. S., 1997. Metal fume fever: characterization of clinical and plasma IL-6 responses in controlled human exposures to zinc oxide fume at and below the threshold limit value. *Journal of Occupational and Environmental Medicine* 39, 722-726.
- Gurr, J. R., Wang, A. S., Chen, C. H., and Jan, K. Y., 2005. Ultrafine titanium dioxide particles in the absence of photoactivation can induce oxidative damage to human bronchial epithelial cells. *Toxicology* 213, 66-73.
- Hintze, K. J., Wald, K. A., Zeng, H., Jeffery, E. H., and Finley, J. W., 2003. Thioredoxin reductase in human hepatoma cells is transcriptionally regulated by sulforaphane and other electrophiles via an antioxidant response element. *Journal of Nutrition* 133, 2721-2727.
- Huang, G. G., Wang, C. T., Tang, H. T., Huang, Y. S., and Yang, J., 2006. ZnO nanoparticle-modified infrared internal reflection elements for selective detection of volatile organic compounds. *Analytical Chemistry* 78, 2397-2404.
- Jeng, H. A., and Swanson, J., 2006. Toxicity of metal oxide nanoparticles in mammalian cells. *Journal of Environmental Science and Health, Part A Toxic/Hazardous Substances and Environmental Engineering* 41, 2699-2711.
- Jeong, W., Park, S. J., Chang, T. S., Lee, D. Y., and Rhee, S. G., 2006. Molecular mechanism of the reduction of cysteine sulfinic acid of peroxiredoxin to cysteine by mammalian sulfiredoxin. *Journal of Biochemical Chemistry* 281, 14400-14407.
- Kang, J. L., Moon, C., Lee, H. S., Park, E. M., Kim, H. S., and Castranova, V., 2008. Comparison of the Biological Activity between Ultrafine and Fine Titanium Dioxide Particles in RAW 264.7 Cells Associated with Oxidative Stress. *Journal*

- of Toxicological Environmental Health 71, Part A, 478-485.
- Kipen, H. M., and Laskin, D. L., 2005. Smaller is not always better: nanotechnology yields nanotoxicology. *American Journal of Physiology* 289, L696-697.
- Lewinski, N., Colvin, V., and Drezek, R., 2008. Cytotoxicity of nanoparticles. *Small* (Weinheim an der Bergstrasse, Germany) 4, 26-49.
- Li, N., Sioutas, C., Cho, A., Schmitz, D., Misra, C., Sempf, J., Wang, M., Oberley, T., Froines, J., and Nel, A., 2003. Ultrafine particulate pollutants induce oxidative stress and mitochondrial damage. *Environmental Health Prospect* 111, 455-460.
- Lin, W., Huang, Y. W., Zhou, X. D., and Ma, Y., 2006a. In vitro toxicity of silica nanoparticles in human lung cancer cells. *Toxicology Applied Pharmacology*. 217, 252-259. DOI: 10.1016/j.taap.2006.10.004.
- Lin, W., Huang, Y. W., Zhou, X. D., and Ma, Y., 2006b. Toxicity of cerium oxide nanoparticles in human lung cancer cells. *International Journal of Toxicology* 25, 451-457.
- Lin, W., Isaac, S., Huang, Y. U., Zhou, X. D., and Ma, Y. F., 2008a. Cytotoxicity and cell membrane depolarization induced by aluminum oxide nanoparticles in human lung epithelial cells A549. *Toxicological and Environmental Chemistry* 90, 983-996. DOI: 10.1080/02772240701802559.
- Lin, W., Xu, Y., Huang, C. C., Ma, Y. F., Shannon, K. B., Chen, D. R., and Huang, Y. W., 2008b. Toxicity of Nano- and Micro-sized ZnO Particles in Human Lung Epithelial Cells. *Journal of Nanoparticle Research* 11:25-39. DOI 10.1007/s11051-008-9419-7.
- Moller, W., Brown, D. M., Kreyling, W. G., and Stone, V., 2005. Ultrafine particles cause

cytoskeletal dysfunctions in macrophages: role of intracellular calcium. Part.

Fibre Toxicology 2, 7.

Nel, A., Xia, T., Madler, L., and Li, N., 2006. Toxic potential of materials at the nanolevel.

Science 311, 622-627.

Oberdorster, G., Oberdorster, E., and Oberdorster, J., 2005. Nanotoxicology: an emerging discipline evolving from studies of ultrafine particles. *Environmental Health*

Perspect 113, 823-839.

Park, E. J., Yi, J., Chung, K. H., Ryu, J. C., Park, K., 2008. Oxidative stress and apoptosis induced by titanium dioxide nanoparticles in cultured BEAS-2B cells. *Toxicology*

Letters 180, 222-229.

Prahalad, A. K., Inmon, J., Dailey, L. A., Madden, M. C., Ghio, A. J., and Gallagher, J. E., 2001. Air pollution particles mediated oxidative DNA base damage in a cell free system and in human airway epithelial cells in relation to particulate metal content and bioreactivity. *Chemistry Research Toxicology* 14, 879-887.

Ramakrishna, G. G., H. N., 2003. Effect of particle size on the reactivity of quantum size ZnO nanoparticles and charge-transfer dynamics with adsorbed catechols.

Langmuir 19, 3006-3012.

Sarkar, S., Sharma, C., Yog, R., Periakaruppan, A., Jejelowo, O., Thomas, R., Barrera, E.

V., Rice-Ficht, A. C., Wilson, B. L., and Ramesh, G. T., 2007. Analysis of stress responsive genes induced by single-walled carbon nanotubes in BJ Foreskin cells.

J. Nanoscience and Nanotechnology 7, 584-592.

Sharma, S., Wyatt, G. P., and Steele, V. E., 1997. A carcinogen-DNA binding assay as a biomarker screen for identifying potential chemopreventive agents. *Methods in*

Cell Science 19, 45-48.

- Timblin, C. R., Shukla, A., Berlinger, I., Berube, K. A., Churg, A., and Mossman, B. T., 2002. Ultrafine airborne particles cause increases in protooncogene expression and proliferation in alveolar epithelial cells. *Toxicology and Applied Pharmacology*. 179, 98-104.
- Vassallo, N., and Herms, J., 2003. Cellular prion protein function in copper homeostasis and redox signalling at the synapse. *J J. NeuroChemistry* 86, 538-544.
- Wagner, A. J., Bleckmann, C. A., Murdock, R. C., Schrand, A. M., Schlager, J. J., and Saber, M. H., 2007. Cellular Interaction of Different Forms of Aluminum Nanoparticles in Rat Alveolar Macrophages. *Journal of Physical Chemistry* 111, 7353-7359.
- Wan, J., Martinvalet, D., Ji, X., Lois, C., Kaech, S. M., Von Andrian, U. H., Lieberman, J., Ahmed, R., and Manjunath, N., 2003. The Bcl-2 family pro-apoptotic molecule, BNIP3 regulates activation-induced cell death of effector cytotoxic T lymphocytes. *Immunology* 110, 10-17.
- White, A. R., Collins, S. J., Maher, F., Jobling, M. F., Stewart, L. R., Thyer, J. M., Beyreuther, K., Masters, C. L., and Cappai, R., 1999. Prion protein-deficient neurons reveal lower glutathione reductase activity and increased susceptibility to hydrogen peroxide toxicity. *American Journal of Pathology*. 155, 1723-1730.
- Xia, T., Kovoichich M., Liong, M., Madler L., Gilbert, B., Shi, H., Yeh, J.I., Zink, J.I. and Nel, A.E., 2008. Comparison of the Mechanism of Toxicity of Zinc Oxide and Cerium Oxide Nanoparticles Based on Dissolution and Oxidative Stress Properties. *ACS NANO* 10, 2121-2134.

Zhu, B. L., Xie, C. S., Zeng, D. W., Song, W. L., and Wang, A. H., 2005. Investigation of gas sensitivity of Sb-doped ZnO nanoparticles. *Material Chemistry Physics* 89, 148-153.

Table 1.1. Metal impurity levels of 20 nm ZnO particles in dry powder. The detection limit of the inductively-coupled plasma-mass spectrometry (ICP-MS) system was 0.04 ppm.

Elements	Metal Impurity (ppm)	Highest working conc. ($\mu\text{g/ml}$)
Sr	18,900	0.189
Cd	1,700	0.017
Be, Fe, V, Mn, Co, Na, Mo, Cs, Ti, U, Na, K, Cu, Se, Ca, As, Pb, Mg, Ga, Al, Sb, Ti, Ni, Ag, Ba, Rb, Cr	Not detected	Not detected
Total	20,600	0.206

Table 1.2. ZnO-mediated changes in cellular pathway-specific gene expression associated with oxidative stress and antioxidant defense in BEAS-2B cells.

Position	GeneBank	Description	Fold change	Class*
A01	NM_000477	Albumin	0.65	4
A02	NM_000697	Arachidonate 12-lipoxygenase	1.09	1,3
A04	NM_001159	Aldehyde oxidase 1	0.85	1
A05	NM_000041	Apolipoprotein E	0.67	4
A06	NM_004045	ATX1 antioxidant protein 1 homolog	1.37	4
A07	NM_004052	BCL2/adenovirus E1B interacting	3.59	6
A08	NM_001752	Catalase	0.94	3
A09	NM_002985	Chemokine (C-C motif) ligand 5	0.65	5
A10	NM_005125	Copper chaperone for superoxide	1.14	1
A11	NM_007158	Cold shock domain containing E1,	1.12	4
A12	NM_000101	Cytochrome b-245, alpha polypeptide	0.52	1
B01	NM_134268	Cytoglobin	0.59	1
B02	NM_001013742	Diacylglycerol kinase, kappa	0.64	4
B03	NM_014762	24-dehydrocholesterol reductase	1.73	3, 6
B04	NM_175940	Dual oxidase 1	0.55	1, 2, 3
B05	NM_014080	Dual oxidase 2	0.68	1, 2, 3
B06	NM_004417	Dual specificity phosphatase 1	0.62	4, 7
B07	NM_001979	Epoxide hydrolase 2, cytoplasmic	0.62	3
B08	NM_000502	Eosinophil peroxidase	0.57	2
B09	NM_021953	Forkhead box M1	0.91	7
B10	NM_197962	Glutaredoxin 2	1.46	1, 6
B11	NM_153002	G protein-coupled receptor 156	0.83	2, 3
B12	NM_000581	Glutathione peroxidase 1	1.19	2, 3
C01	NM_002083	Glutathione peroxidase 2	0.7	2, 3
C02	NM_002084	Glutathione peroxidase 3	0.91	2, 3
C03	NM_002085	Glutathione peroxidase 4	0.92	2, 3
C04	NM_001509	Glutathione peroxidase 5	0.66	2, 3
C05	NM_182701	Glutathione peroxidase 6	0.65	2, 3
C06	NM_015696	Glutathione peroxidase 7	0.77	2, 3
C07	NM_000637	Glutathione reductase	1.45	2, 3
C08	NM_000178	Glutathione synthetase	0.91	4
C09	NM_001513	Glutathione transferase zeta 1	0.92	2, 3
C10	NM_001518	General transcription factor II, i	0.75	1
C12	NM_006151	Lactoperoxidase	0.61	2, 3
D01	NM_000242	Mannose-binding lectin (protein C) 2	0.59	5
D02	NM_004528	Microsomal glutathione S-transferase	1.13	2
D03	NM_000250	Myeloperoxidase	0.62	2, 3
D04	NM_002437	MpV17 mitochondrial inner membrane	1.16	1

Table 1.2. Continued

Position	GeneBank	Description	Fold change	Class*
D05	NM_012331	Methionine sulfoxide reductase A	1.33	3
D06	NM_005954	Metallothionein 3	1.23	4
D07	NM_004923	Metallothionein-like 5	1.07	4
D08	NM_000265	Neutrophil cytosolic factor 1	0.55	1
D09	NM_000433	Neutrophil cytosolic factor 2	0.59	1
D10	NM_003551	Non-metastatic cells 5	0.76	7
D11	NM_000625	Nitric oxide synthase 2A	0.62	3
D12	NM_024505	NADPH oxidase	0.67	1
E01	NM_002452	Nudix-type motif 1	1	4
E02	NM_181354	Oxidation resistance 1	0.88	4
E03	NM_005109	Oxidative-stress responsive 1	0.66	4
E04	NM_020992	PDZ and LIM domain 1 (elfin)	1.14	4
E06	NM_007254	Polynucleotide kinase 3'-phosphatase	0.5	4
E07	NM_002574	Peroxiredoxin 1	1.54	2, 3
E08	NM_005809	Peroxiredoxin 2	0.97	2, 3
E09	NM_006793	Peroxiredoxin 3	13.36	2, 3
E10	NM_006406	Peroxiredoxin 4	1.49	2, 3
E11	NM_181652	Peroxiredoxin 5	1.1	2, 3
E12	NM_004905	Peroxiredoxin 6	1	2, 3
F01	NM_020820	PIP3-dependent RAC exchanger 1	0.72	1
F02	NM_006093	Proteoglycan 3	0.64	4
F03	NM_183079	Prion protein (p27-30)	5.72	4
F04	NM_000962	Prostaglandin-endoperoxide synthase 1	0.62	2
F05	NM_000963	Prostaglandin-endoperoxide synthase 2	0.59	2
F06	NM_012293	Peroxidasin homolog (Drosophila)	0.99	2
F07	NM_144651	Peroxidasin homolog (Drosophila)-like	0.76	2
F08	NM_014245	Ring finger protein 7	1.17	4
F09	NM_182826	Scavenger receptor class A, member 3	0.45	4
F10	NM_203472	Selenoprotein S	0.92	4
F11	NM_005410	Selenoprotein P, plasma, 1	0.96	4
F12	NM_003019	Pulmonary-associated protein D	0.74	1, 5
G01	NM_016276	Serum/glucocorticoid regulated kinase	0.63	3, 7
G02	NM_012237	Sirtuin 2	0.64	4, 6
G03	NM_000454	Superoxide dismutase 1	1.33	1, 3
G04	NM_000636	Superoxide dismutase 2	0.89	1, 3
G05	NM_003102	Superoxide dismutase 3	1.1	1, 3
G06	NM_080725	Sulfiredoxin 1 homolog (S. cerevisiae)	0.75	3, 4
G07	NM_006374	Serine/threonine kinase 25	0.52	4
G08	NM_000547	Thyroid peroxidase	0.72	2, 3
G09	NM_003319	Titin	0.72	2

Table 1.2. Continued

Position	GeneBank	Description	Fold change	Class*
G10	NM_032243	Thioredoxin domain-containing 2	0.9	3
G11	NM_003330	Thioredoxin reductase 1	2.76	3
G12	NM_006440	Thioredoxin reductase 2	1	3

* 1=Genes involved in superoxide release and metabolism; 2=Genes with peroxidase activity; 3=Genes with oxidoreductase activity; 4=Other genes involved in oxidative stress; 5=Inflammation relevant genes; 6=Apoptosis inducers; 7=Cell division relevant genes.

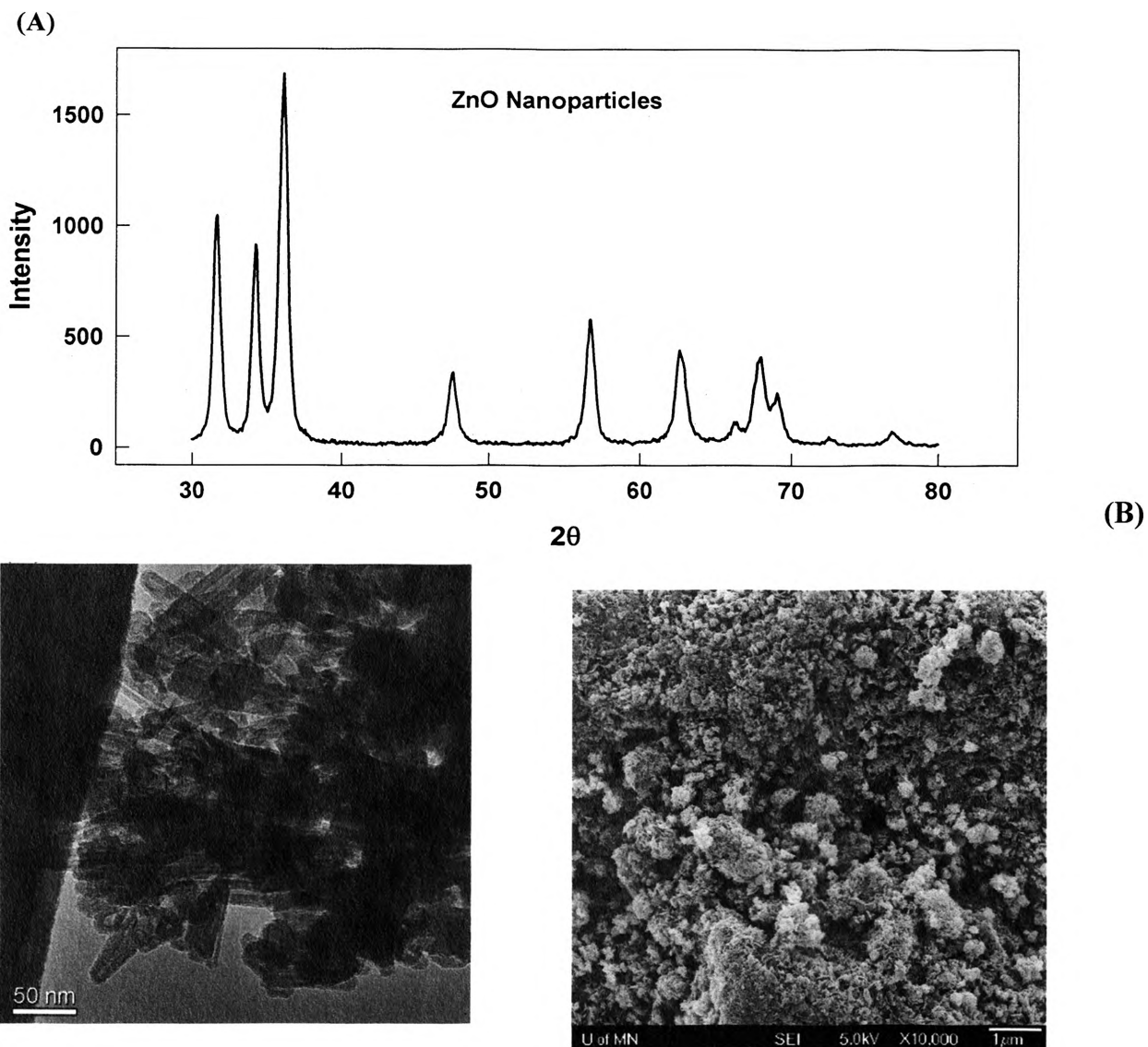
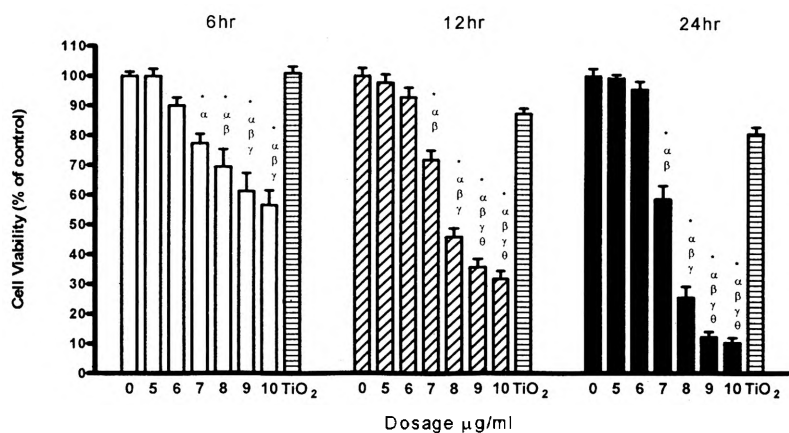


Figure 1.1. (A) X-ray diffractometry, (B) transmission electron microscopy (TEM) and (C) scanning electron microscopy (SEM) of 20 nm ZnO particles.

(A)



(B)

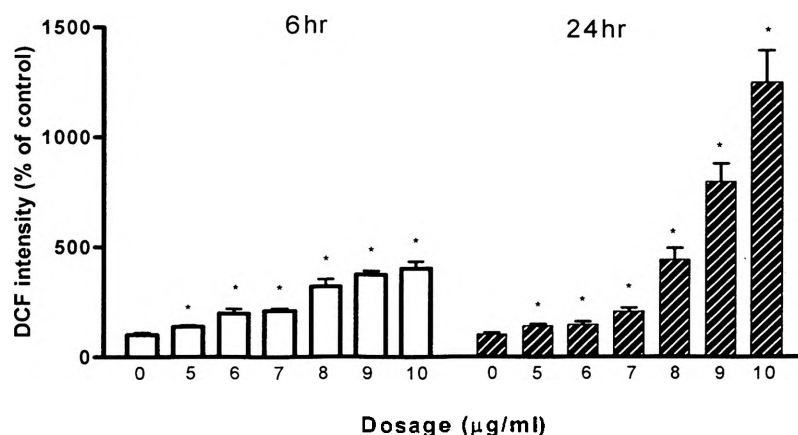


Figure 1.2. (A) Time- and dosage-dependent cytotoxicity of 20 nm ZnO particles constructed by MTS assay. Titanium dioxide at 20 µg/ml was used for comparison. (B) Oxidative stress induced by exposure of BEAS-2B cells to ZnO. After cells were exposed to ZnO for 6 or 24hours, as indicated, intracellular ROS levels were measured and normalized by the corresponding cell numbers. ZnO significantly elevated the intracellular ROS at all concentration levels examined. Significance is indicated by: * $p < 0.05$ vs. control cells; ^α $p < 0.05$ vs. cells exposed to 5 µg/ml; ^β $p < 0.05$ vs. cells exposed to 6 µg/ml; ^γ $p < 0.05$ vs. cells exposed to 7 µg/ml; ^δ $p < 0.05$ vs. cells exposed to 8 µg/ml.

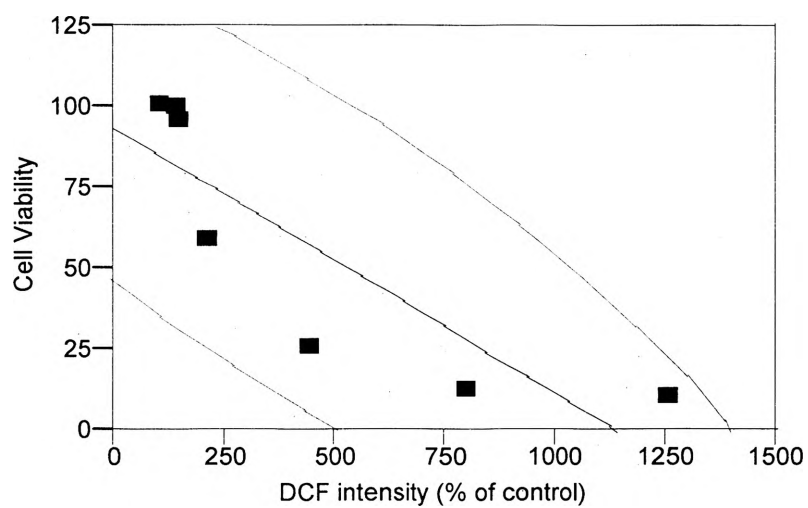


Figure 1.3. An inverse correlation ($R^2=0.741$) between ROS and viability of BEAS-2B cells exposed to ZnO for 24 h. Green lines indicate bivariate normal ellipse $p = 0.950$.

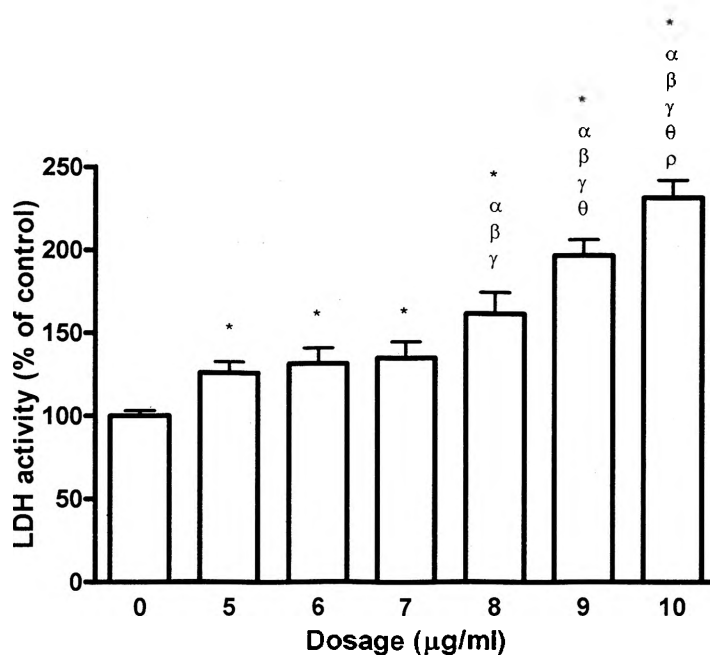


Figure 1.4. LDH activities in the BEAS-2B cell culture medium following a 24 h exposure to ZnO. The means \pm SD from three independent experiments performed in triplicate are shown. * $p < 0.05$ vs. control cells; $^{\alpha}p < 0.05$ vs. cells exposed to 5 $\mu\text{g/ml}$; $^{\beta}p < 0.05$ vs. cells exposed to 6 $\mu\text{g/ml}$; $^{\gamma}p < 0.05$ vs. cells exposed to 7 $\mu\text{g/ml}$; $^{\theta}p < 0.05$ vs. cells exposed to 8 $\mu\text{g/ml}$; $^{\rho}p < 0.05$ vs. cells exposed to 9 $\mu\text{g/ml}$.

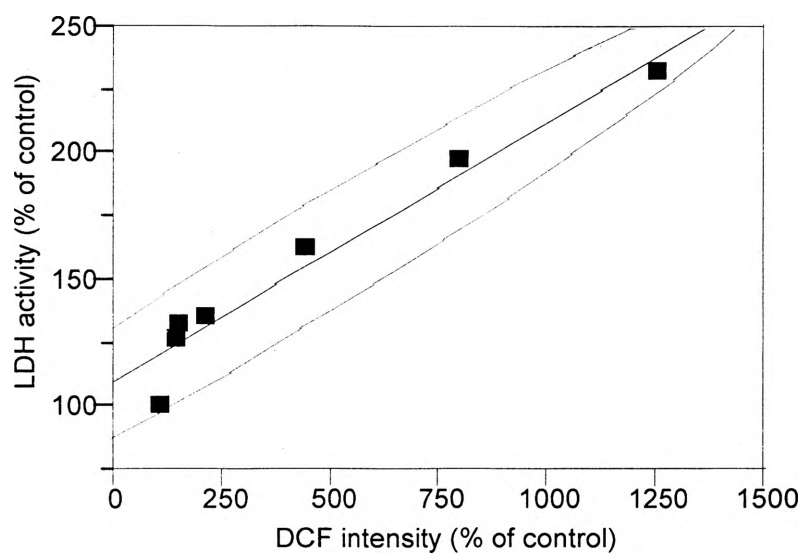


Figure 1.5. Positive correlation ($R^2=0.953$) between LDH activity and ROS intensity of BEAS-2B cells exposed to ZnO for 24 hours. Green lines indicate bivariate normal ellipse $p = 0.950$.

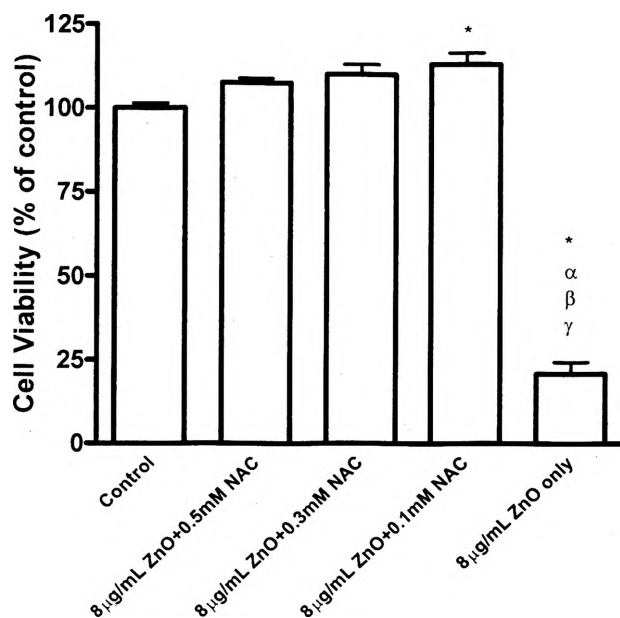


Figure 1.6. The influence of the antioxidant N-acetylcysteine (NAC) on the reduction in cell viability caused by exposure to ZnO. Cells were incubated with 8 µg/ml ZnO with or without NAC for 24 h. Values are mean ± SD from three independent experiments each performed in triplicate. Significance: * $p < 0.05$ vs. cells exposed to control cells; ^α $p < 0.05$ vs. cells exposed to 0.5 mM; ^β $p < 0.05$ vs. cells exposed to 0.3 mM; ^γ $p < 0.05$ vs. cells exposed to 0.1 mM.

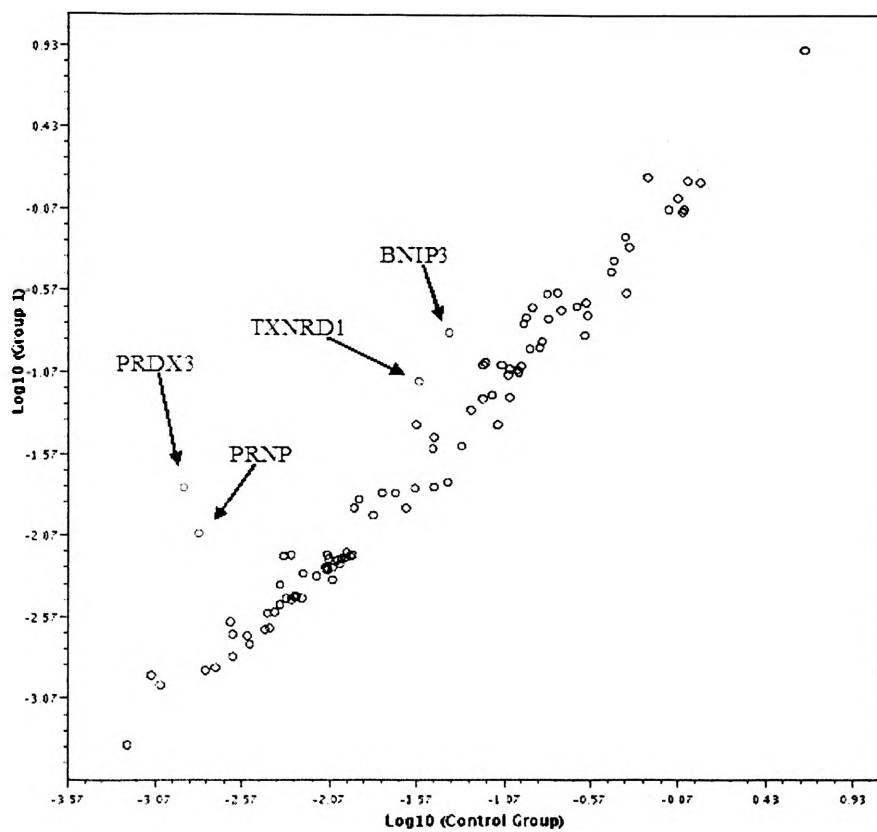


Figure 1.7. Gene expression patterns in the BEAS-2B cells treated with 5 $\mu\text{g/ml}$ of 20nm ZnO for 24 hr. Red spots indicate the genes that were changed by at least 2.5 fold.

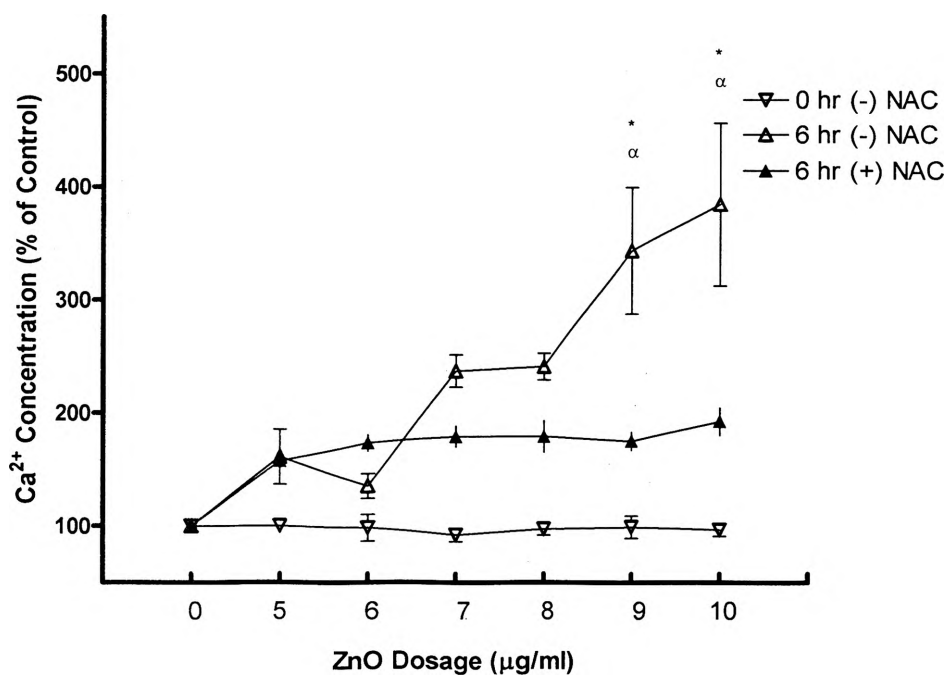


Figure 1.8. Influence of ZnO nanoparticles on intracellular calcium concentrations.

Calcium concentrations were measured immediately (0 h) or 6 h after exposure to Zn at the indicated concentration. NAC was included in one 6 h exposure group, as indicated.

* $p < 0.05$ shows the significantly difference between 6 h (-)NAC and 6h (+)NAC.

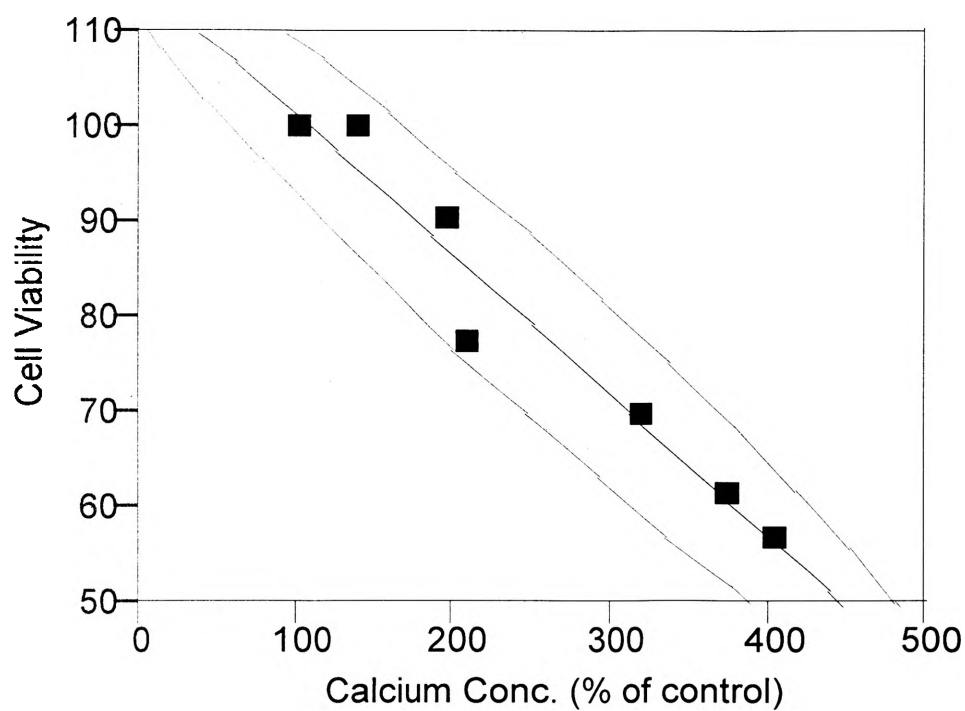


Figure 1.9. The inverse relationship ($R^2=0.952$) between intracellular calcium levels and cell viability in ZnO-exposed BEAS-2B cells, green lines indicate bivariate normal ellipse $p = 0.950$.

VITA

Chuan-Chin Huang was born in Taipei, Taiwan on April 22th, 1981. He finished the Bachelor's degree from Zoology Department at Nation Taiwan University in 2002. She completed his first Master's degree from Institution of Ecology and Evolutionary Biology at National Taiwan University. In May 2007, he joined Missouri University of Science and Technology in 2007. As a master's degree student, he worked in Dr. Yue-wern Huang's lab for two years and received his second Master's degree in Applied Environmental Biology from Missouri University of Science and Technology on May, 2009.